Transient Phenomena in the Pulse Radiolysis of Oxoisoaporphine Derivatives in Acetonitrile

Julio R. De la Fuente,*,† Gabriel Kciuk,‡ Eduardo Sobarzo-Sanchez,§ and Krzysztof Bobrowski‡

Departamento de Química Orgánica y Fisicoquímica, Facultad de Ciencias Químicas y Farmacéuticas, Universidad de Chile, Casilla 223, Santiago 1, Chile, Institute of Nuclear Chemistry and Technology, 03-195 Warsaw, Poland, and Departamento de Química Orgánica, Facultad de Farmacia, Universidad de Santiago de Compostela, Santiago de Compostela, Spain

The absorption-spectral and kinetic behavior of radical ions and triplet states of two oxoisoaporphine derivatives, 2,3-dihydrooxoisoaporphine (2,3-DHOA) and 5-methoxy-2,3-dihydrooxoisoaporphine (5-MeO-2,3-DHOA), have been studied by UV−vis spectrophotometric pulse radiolysis in a neat acetonitrile saturated with argon and oxygen at room temperature. The radical anions of 2,3-DHOA and 5-MeO-2,3-DHOA are characterized by intense absorption maxima located at $\lambda_{max} = 605$ and 590 nm, with molar absorption coefficients $\epsilon_{605} = 5600\ M^{-1}\ cm^{-1}$ and $\epsilon_{590} = 4900\ M^{-1}\ cm^{-1}$, respectively. Both radical anions decay via first-order kinetics with the rate constants in the range $(1.5-2.6) \times 10^5\ s^{-1}$, predominantly through protonation by adventitious water forming neutral-hydrogenated radicals. Oxygen insensitive, the radical cations of 2,3-DHOA are characterized by a strong nondescript absorption band with no distinct λ_{max} in the range 350−450 nm. On the other hand, the radical cations of 5-MeO-2,3-DHOA are characterized by the distinctive absorption band with $\lambda_{max} = 420$ nm. The experimental spectra of the neutral-hydrogenated radicals and the triplet excited states derived from 2,3-DHOA and 5-MeO-2,3-DHOA are in accordance with the spectra observed previously during laser flash photolysis (De la Fuente, J. R.; et al. *J. Phys. Chem.* 2005, *109*, 5897). Most of the transient spectra generated radiolytically are adequately reproduced by quantum mechanical semiempirical PM3 and ZINDO/S methods.

Introduction

Oxoisoaporphines are a family of oxoisoquinoline-derived alkaloids that have been isolated from *Menispermaceae* as natural source.[1] In traditional Chinese medicine the rhizomes of the plants are used as an analgesic and antipyretic Cytotoxic activity of the extracts from these plants has been also reported.[2−4] It has been claimed that these compounds could be phytoalexins generated by plants against pathogen infections.[5]

Several years ago, we undertook a detailed study of photoreduction of synthetic derivatives of oxoisoaporphines by tertiary amines.[6−8] It was found that photoreduction of 5,6-dimethoxy-, 5-methoxy- (A2), and 2,3-dihydro-7*H*-dibenzo[*de*,*h*]quinolin-7-ones (A1) (Chart 1), by tertiary amines in oxygen-free solutions occurs via the formation of the radical anion ($A^{\bullet-}$, Chart 1)), the neutral-hydrogenated radical ($ANH^{\bullet}$, Chart 1) and the long-lived semireduced metastable ion (ANH^-, Chart 1), eventually. The mechanism is a stepwise electron−proton−electron transfer with a limiting quantum yield approaching 0.1 at high amine concentrations.[6]

The mechanism proposed[6] involves the formation of the radical ion pair complex by the one-electron transfer from the amine to the excited triplet of the oxoisoaporphine (reaction 1). Within the radical ion pair complex, a feasible donation of a proton by the amine radical cation to the radical anion of the oxoisoaporphine leads to the formation of the hydrogenated neutral radical of the oxoisoaporphine $ANH^{\bullet}$ (reaction 2). The latter radical undergoes a second electron transfer from the more reductive imine radical, leading to the N-hydrogen anion of the oxoisoaporphine, ANH^-, and the iminium cation (reaction 3).

$$^3A^* + R_2N{-}CH_2R' \rightarrow [A^{\bullet-} \cdots R_2N^{\bullet+}{-}CH_2R'] \quad (1)$$

$$[A^{\bullet-} \cdots R_2N^{\bullet+}{-}CH_2R'] \rightarrow ANH^{\bullet} + R_2N{-}C^{\bullet}HR' \quad (2)$$

$$ANH^{\bullet} + R_2N{-}C^{\bullet}HR' \rightarrow ANH^- + R_2N^+{=}CHR' \quad (3)$$

The photoreduction mechanism was elaborated on the basis of spectral identification of all the intermediates involved in the photoreduction process. They were generated by laser flash photolysis of the respective oxoisoaporphines in the presence of suitable amines that were capable or not capable to donate hydrogen.[7] To supplement spectral assignments of the intermediates, computations by using ZINDO/S semiempirical quantum mechanical methods on the PM3 optimized structures of transient species have been also performed.[7] Comparison of the calculated and experimental spectra was helpful to show that the photoinduced electron transfer (PET) from the amines to the oxoisoaporphine generates contact radical ion pair complexes with the distance between the amine N atom and the O atom in the >C=O group of the oxoisoaporphine near to 2.5 Å. The calculated spectra of these contact ion radical pair complexes are characterized by the strongest electronic transitions close to the experimentally observed maxima of the absorption bands located at $\lambda = 490$ nm.[7] On the other hand, the calculated spectra of the isolated radical-anions generate the strongest electronic transition near $\lambda = 600$ nm, the value which was not reflected in the experimentally observed absorption spectra. Therefore,

* Corresponding author. Fax: (56-2)-978-2868. E-mail: jrfuente@ciq.uchile.cl.
† Universidad de Chile.
‡ Institute of Nuclear Chemistry and Technology.
§ Universidad de Santiago de Compostela.

CHART 1: Structures of Oxoisoaporphines under Study (A) and the Respective Radical Ions ($A^{\bullet -}$ and $A^{\bullet +}$), Neutral Radicals, ($ANH^{\bullet}$), and the N-Hydrogen Anions (ANH^{-}) Derived from Them

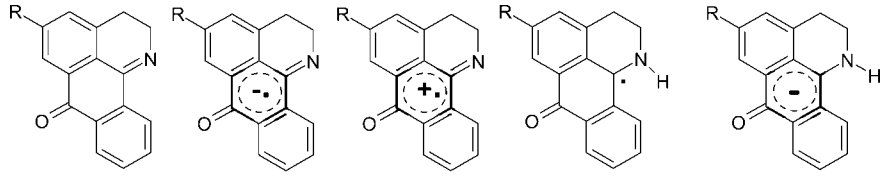

A1: R = H-
A2: R = MeO-

it was concluded that the observation of isolated oxoisoaporphine radical anions is not possible in the systems containing amines.

To overcome this problem, another experimental approach has been applied in this work, namely the pulse radiolysis technique.[9−11] Pulse radiolysis offers a convenient method of generation of radical ions and excited states or preferentially one of them, depending on the solvent used.[10] Therefore, one may, by choice of a solvent, and in addition, of a saturating gas, exercise some control over the nature of the ionic species and excited states formed in the irradiated solvents and thus selectively generate radical ions and/or excited states derived from the solutes.[12−16]

In the present study we generated and identified radical ions and triplet states derived from two oxoisoaporphines in acetonitrile. Acetonitrile is known for pulse radiolytic generation of cation as well as anion precursors (see Radiolysis of Acetonitrile in the Experimental Section).[14,15,17−22] We have initiated primarily this study to generate isolated oxoisoaporphine radical anions and to study their spectra and kinetic behavior, and further to confront them with the spectra calculated previously using ZINDO/S semiempirical quantum mechanical methods.[7] In addition, knowledge regarding the spectral and kinetic behavior of oxoisoaporphine radical cations and triplet excited states will become necessary in interpreting some of the transient phenomena observed by us in the pulse radiolysis of these systems in various solvents. Furthermore, using two oxoisoaporphines without and with the methoxy group ($-OCH_3$), we have examined effects of the electron-donating substitution on absorption maxima of radical ions and their stability.

Experimental Section

Materials. Acetonitrile was purchased from J. T. Baker with 99.9% purity (Baker HPLC analyzed), and was used as received.

Synthesis of Oxoisoaporphines. A1 and A2 were obtained by the procedure reported by Favre et al.[23] and by Walker et al.,[24] and completely characterized as reported previously.[25]

Preparation of Solutions. All solutions for pulse radiolysis experiments were prepared freshly before experiments with organic solvent and contained 0.1 mM of oxoiso-aporphines. Solutions were subsequently purged for at least 30 min per 200 mL of sample with the desired gas (Ar or O_2) before pulse irradiation. All solutions containing 5-methoxy-2,3-dihydrooxoisoaporphine for laser flash photolysis experiments were prepared with absorbance between 0.2−0.6 at the excitation wavelength 355 nm and were purged with nitrogen for a 20 min in a 10 mm quartz cell sealed with a septum. Immediately after purging, an aliquot of diluted triethylamine (TEA) was added through the septum for the spectral experiments. Transient spectra with the presence of TEA were monitored typically with not more than four laser pulses for each monitored wavelength and by taking 10 min intervals between each wavelength.

Pulse Radiolysis. Pulse radiolysis experiments were performed with the INCT LAE 10 linear accelerator with typical pulse lengths of 7−10 ns. The data acquisition system allows for kinetic traces to be displayed on multiple time scales. A detailed description of the experimental setup for optical measurements has been given elsewhere along with the basic details of the equipment and the data collection system.[26,27] The irradiation cell was supplied with a fresh solution by continuous and controlled flow. The dose per pulse, which was determined by thiocyanate dosimetry, was on the order of 18−20 Gy (1 Gy = 1 J kg^{-1}). Radiolytic yields are given in SI units as μmol J^{-1}, i.e., the number of product species in micromoles that are generated for every joule of energy absorbed by the solution.

All experiments were performed with a continuous flow of sample solutions at room temperature (∼20 °C). Experimental error limits are ±10% unless specifically noted.

Laser Flash Photolysis. Laser flash photolysis experiments were performed with a Q-switched Nd:YAG laser, Quantel Brilliant with the excitation at 355 nm. The flash photolysis setup was described previously.[28,29]

Quantum mechanical calculations were made using a Windows version of HyperChem-6.01 by HyperCube, Inc. in a compatible personal computer with an Intel Pentium 4 processor of 2.0 GHz with 512 MB of RAM. Calculated spectra employing the PM3 minimized geometries for isolated $A^{\bullet +}$ cations were obtained by using ZINDO/S, considering the first five unoccupied and five occupied MO with weighting factor values of 1.267 and 0.585 for $\sigma-\sigma$ and $\pi-\pi$ overlap respectively. By including more MO (10 + 10) a greater number of absorption lines in the high-energy region beyond the range of measurements were obtained, however, without affecting the spectral region of interest in this study. Optimized geometries were calculated by using PM3 semiempirical method with UHF optimization with the proper charge and multiplicity (+1, 2) disregarding any solvent effect. The starting point for the optimization was the ground state of the respective species. The dipole moments were also obtained for these species from the PM3 optimization.

Radiolysis of Acetonitrile. Pulse irradiation of a neat acetonitrile leads to the formation of the acetonitrile positive ions and electrons/negative ions (eqs 4 and 5), and triplet states formed by solute radical ion recombination (eqs 6 and 7). Low yields of G (∼0.2) for the oxidizing species[20] and G (∼0.3) for the triplets[22,30] were measured. On the other hand the yield of

reducing species was found to be in the range of $G = 1.03-1.55$.[18,30]

$$CH_3CN \sim\sim\rightarrow CH_3CN^{\bullet+} + e^-_{solv} \quad (4)$$

$$e^-_{solv} + CH_3CN \rightarrow CH_3CN^{\bullet-} \quad (5)$$

$$CH_3CN^{\bullet+} + CH_3CN^{\bullet-} \rightarrow 2^3CH_3CN^* \quad (6)$$

$$CH_3CN^{\bullet+} + e^-_{solv} \rightarrow {}^3CH_3CN^* \quad (7)$$

In this solvent saturated with Ar both radical ions can be formed according to eqs 8−10, whereas in O_2-saturated solution only radical cations of a solute are formed according to eq 10 (ionization potential of CH_3CN is ≈12 eV).[31]

Solute radical anions are not formed because their precursors, solvated electrons and/or solvent radical anions, are scavenged by O_2 (eq 11).

$$e^-_{solv} + S \rightarrow S^{\bullet-} \quad (8)$$

$$CH_3CN^{\bullet-} + S \rightarrow CH_3CN + S^{\bullet-} \quad (9)$$

$$CH_3CN^{\bullet+} + S \rightarrow CH_3CN + S^{\bullet+} \quad (10)$$

$$e^-_{solv}/CH_3CN^{\bullet-} + O_2 \rightarrow O_2^{\bullet-} + CH_3CN \quad (11)$$

Oxygen also serves as a strong quencher for triplets of solutes and solvents.

Results

2,3-Dihydrooxoisoaporphine. ***Argon-Saturated Solutions.*** Pulse radiolysis of a solution of 2,3-dihydrooxoisoaporphine (A1, Chart 1) in argon-saturated acetonitrile yielded a complex series of spectral changes (Figure 1A).

A broad absorption was observed at 50 ns after the pulse in the 350−520 nm range with $\lambda_{max} = 450$ nm and with one distinct absorption band with $\lambda_{max} = 605$ nm (Figure 1A, curve a (□)). Both absorptions build up within <1 μs time domain; however, the growth at $\lambda_{max} = 605$ nm was more pronounced, and after 1 μs after the pulse, the transient absorption spectrum is dominated by the 605 nm band (Figure 1A, curve b (○)). Similarly, the kinetic decays of the 450 nm and 605 nm species differed. The absorption at 605 nm decayed further by a rapid first-order process with $k = (1.5 \pm 0.02) \times 10^5$ s^{-1} (Figure 1A, left inset). With the 450 nm transient, however, the decay followed rather more complex kinetics (Figure 1A, left inset).

Although the absorption at 450 nm and 605 nm decreased in intensity, the new absorption bands appeared at $\lambda_{max} = 360$, 420, and 500 nm at 10 μs after the pulse (Figure 1A, curve c (◇)). Interestingly, the 420 nm absorption band is stable over the time range in which the 605 nm band has almost disappeared (Figure 1A, left inset). On the other hand, the delayed growths are observed at $\lambda_{max} = 370$ and 500 nm over the 7 and 15 μs time domains, with the first-order rate constants $k = (4.6 \pm 0.4) \times 10^5$ s^{-1} and $(3.3 \pm 0.5) \times 10^5$ s^{-1}, respectively (Figure 1A, left inset). Moreover, the decays observed at $\lambda_{max} = 370$, 420, and 500 nm are characterized by different rates, 420 nm being the slowest one (Figure 1A, right inset). At the time when the 605 nm absorption disappeared completely, the spectrum underwent further changes, and 50 μs after the pulse is characterized by two distinct absorption bands with $\lambda_{max} = 420$ and 500 nm, and a pronounced shoulder near 370 nm (Figure 1A, curve d (Δ)). These two absorption bands with $\lambda_{max} = 420$ and 500 nm are still observed at longer time, i.e., 200 μs after the pulse (Figure 1A, curve e (▽)), when the decay of the 360 nm band was close to the completion. All these observations taken together point out for the existence of several different transients.

Oxygen-Saturated Solutions. To sort out the contributions of individual radical anion/triplet and radical cations, an acetonitrile solution containing 2,3-dihydrooxoisoaporphine (A1, Chart 1) was saturated with oxygen as the scavenger for solvated electrons and solvent/solute radical anions. In the presence of oxygen, the absorption spectra recorded at 50 ns and 1 μs after the pulse reveal different features with comparison to the spectra recorded at the same time under deoxygenated conditions (Figure 1B, curve a (□) and b (○)).

Formation of the absorption band with the maximum at $\lambda_{max} = 605$ nm together with the broad absorption band in the range 400−550 nm was completely suppressed. Therefore, it is reasonable to assume tentatively that the 2,3-dihydrooxoisoaporphine derived radical anions ($A1^{\bullet-}$, Chart 1) and likely triplets ($^3A1^*$) are responsible for the absorption bands suppressed. The absorption spectrum recorded at 10 μs after the pulse exhibits a strong nondescript absorption band with no distinct λ_{max} at wavelengths in the range 350−450 nm, and a weakly pronounced absorption band with a maximum located at $\lambda_{max} = 500$ nm (Figure 1B, curve c). Interestingly, the formation of the 350 nm band is fully developed within the range of 7 μs (Figure 1B, left inset), and the formation kinetics recorded at $\lambda = 350$ nm with $k = (3.8 \pm 0.04) \times 10^5$ s^{-1} matches nearly the formation kinetics of the 360 nm band in Ar-saturated acetonitrile (Figure 1A, left inset) suggesting the same species present in both Ar- and O_2-saturated solutions. Although the absorption in the 350−380 nm range decreased in intensity, the spectrum with a pronounced shoulder located 390−410 nm, and with a distinct, however, not very intense, absorption band at $\lambda_{max} = 500$ nm, was developed after 50 μs after the pulse (Figure 1B, curve d). Similarly, as in Ar-saturated solutions a delayed growth with the first-order rate constant $k = (8.5 \pm 0.04) \times 10^5$ s^{-1} was observed at $\lambda = 500$ nm (Figure 1B, left inset). With the further elapse of time, the spectrum observed after 200 μs after the pulse is characterized by two absorption bands with the maxima located at $\lambda_{max} = 410$ and 500 nm (Figure 1B, curve e). This last observation, taken together with the fact that both formation and decay kinetics observed at $\lambda = 350$ and 500 nm are different, suggests the existence of two different cationic species (Figure 1B, right inset). Reasonably, the radical cation derived from 2,3-dihydrooxoisoaporphine ($A1^{\bullet+}$, Chart 1) might be responsible for the absorption below 390 nm. A reasonably good agreement between experimental and calculated spectra (Table 1) for the radical cation ($A1^{\bullet+}$, Chart 1) was found. The absorption shoulder at <420 nm and the most intense absorption observed experimentally at wavelengths <400 nm were reasonably well reproduced by the calculated electronic transitions (Figure 1B).

Interestingly, a comparison of the formation and decay behaviors at $\lambda = 350$ and 500 nm, might indicate that the radical cation is a precursor of the longer-lived 500 nm species. The assignment of the absorption band with two absorption maxima located at $\lambda_{max} = 410$ and 500 nm is not obvious, although very plausibly, it might be a dimeric radical cation ($(A1)_2^{\bullet+}$) formed as a product of association of radical cations and parent 2,3-dihydrooxoisoaporphine molecules. Formation of such species is well-documented in the literature.[32]

Corrected Spectra To Eliminate Contribution of Radical Cation Species. Subtraction of the absorption spectra obtained in O_2-saturated solutions from the respective absorption spectra obtained in Ar-saturated solutions allows us to take apart the

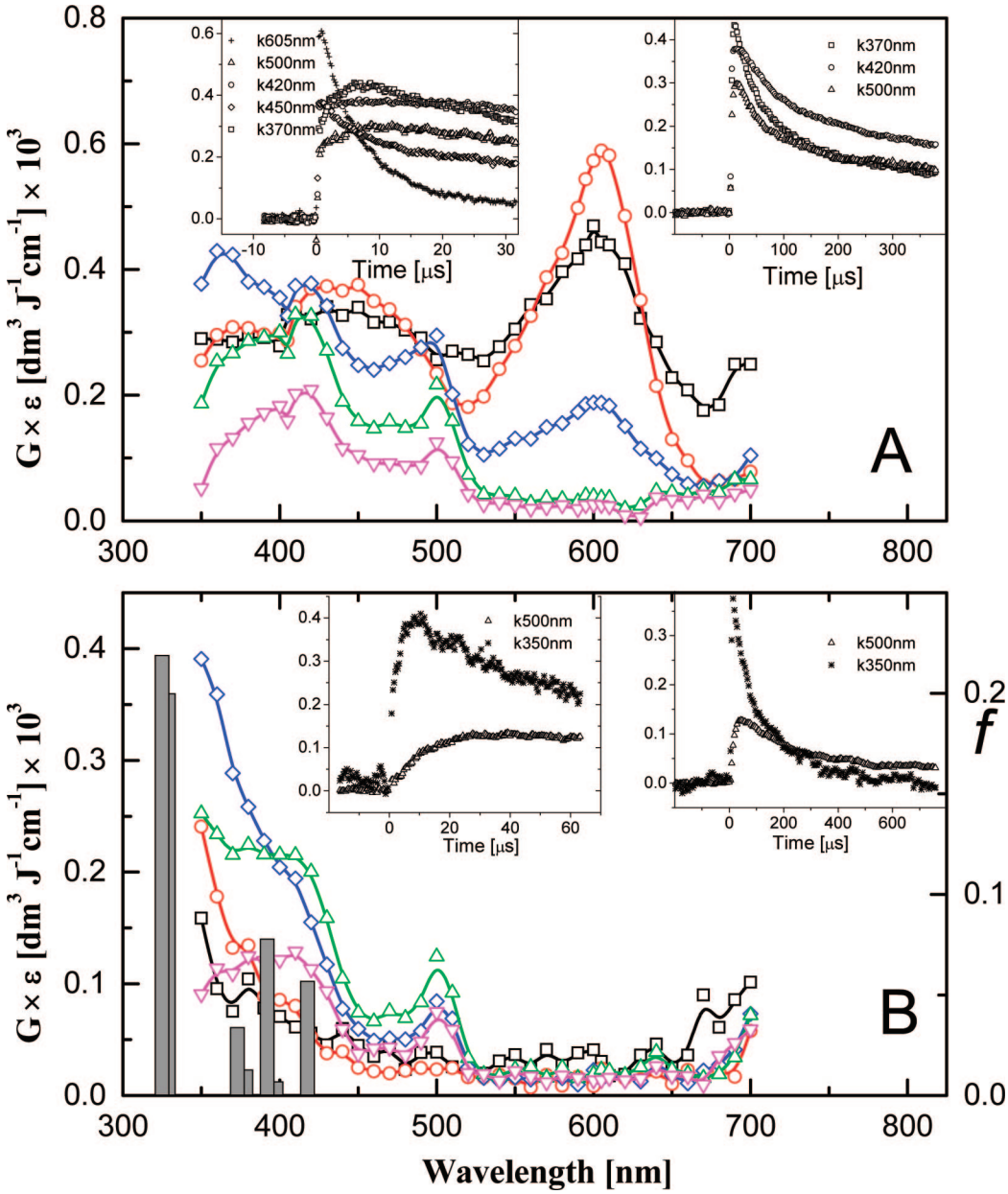

Figure 1. Absorption spectra recorded in (A) Ar-saturated, and (B) O_2-saturated acetonitrile solutions containing 0.1 mM 2,3-dihydrooxoisoaporphine. Spectra were taken after the following time delays: (a) (□) 50 ns; (b) (○) 1 μs; (c) (◇) 10 μs; (d) (Δ) 50 μs; (e) (▽) 200 μs. The shaded vertical bars represent position of the calculated electronic transitions for $A1^{\bullet+}$. The height of the bar is proportional to the oscillator strength (*f*). Insets in (A): short time profiles representing growth and/or decays at λ = 370, 420, 450, 500, and 605 nm (left) and long time profiles representing decays at λ = 370, 420, and 500 nm (right). Insets in (B): short time profiles representing growth and/or decays at λ = 350, and 500 nm (left) and long time profiles representing decays at λ = 350, and 500 nm (right).

contribution of radical cation species, leaving only those absorption spectra that correspond to the radical anions ($A1^{\bullet-}$, Chart 1) and/or the triplets (^{3}A1*) of 2,3-dihydrooxoisoaporphine at shorter times and to the neutral-hydrogenated radical ($A1NH^{\bullet}$, Chart 1), at longer times (Figure 2A).

The corrected absorption spectra recorded 50 ns and 1 μs after the pulse represent combined absorption bands of at least two different species: a radical anion ($A1^{\bullet-}$, Chart 1) with λ_{max} = 605 nm, and a triplet (^{3}A1*) with λ_{max} = 450 nm of 2,3-dihydrooxoisoaporphine (Figure 2A, curves b and c). The position of the absorption maximum of the radical anion ($A1^{\bullet-}$, Chart 1) is in an excellent agreement with the predicted electronic transitions for the radical anion ($A1^{\bullet-}$) (vide infra, Figure 2B) calculated by the ZINDO/S-PM3 method (Table 1).[7] On the other hand, an assignment of the 450 nm band to the triplet (^{3}A1*) is based on the fact that similar absorption band with λ_{max} = 450 nm was obtained by us during the flash photolysis of A1 (Chart 1) and was clearly assigned to the triplet excited state ^{3}A1*.[7]

The contribution of the neutral-hydrogenated radical ($A1NH^{\bullet}$, Chart 1) seems to be already seen at shorter times; however, after a decay of the radical anion ($A1^{\bullet-}$, Chart 1) and a substantial decay of the triplet (^{3}A1*), the absorption spectra recorded after 50 and 200 μs after the pulse (Figure 2A, curves d (Δ) and e (▽)) exhibit the same spectral and kinetic features as the spectrum observed by us during laser flash photolysis of the 2,3-dihydrooxoisoaporphine (A1, Chart 1) in the presence of triethylamine (TEA) (Figure 2A, inset) and are assigned to the neutral-hydrogenated radical ($A1NH^{\bullet}$, Chart 1).[7] Although the fit between experimental and calculated (Table 1) absorption

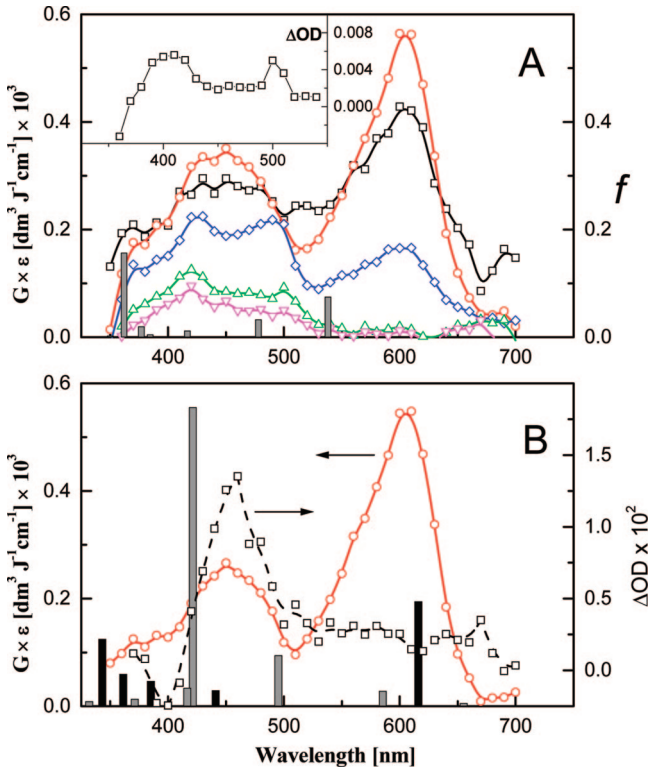

Figure 2. (A) Absorption spectra from the subtraction of the absorption spectra obtained in O_2-saturated solutions from the respective absorption spectra obtained in Ar-saturated solutions at different time delays: (a) (□) 50 ns; (b) (○) 1 μs; (c) (◇) 10 μs; (d) (Δ) 50 μs; (e) (▽) 200 μs. The shaded vertical bars represent position of the calculated electronic transitions for A1NH$^{\bullet}$. The height of the bar is proportional to the oscillator strength (*f*). Inset: absorption spectrum of the neutral-hydrogenated radical (A1NH$^{\bullet}$) obtained by flash photolysis of 2,3-dihydrooxoisoaporphine in N_2-saturated acetonitrile solutions (□).[7] (B) Absorption spectrum from the subtraction of the corrected absorption spectrum at 200 μs (from panel A) from the corrected absorption spectrum at 1 μs (from panel A) (○), and absorption spectrum of the 2,3-dihydrooxoisoaporphine triplet (^{3}A1*) obtained by flash photolysis of 2,3-dihydrooxoisoaporphine in N_2-saturated acetonitrile solutions (□).[7] The vertical bars represent the position of the electronic transition for ^{3}A1* (gray bar) and A1$^{\bullet-}$ (black bar). The height of the bar is proportional to the oscillator strength (*f*).

spectra for the neutral A1NH$^{\bullet}$ (Chart 1) is not very good, the calculated electronic transitions reproduce fairly well the main feature of the experimental spectrum of A1NH$^{\bullet}$ (Chart 1), i.e., the presence of two separated absorption bands, one with the maximum in the UV, and the second one in the visible region (Figure 2A).

Corrected Spectra To Eliminate Contribution of Long-Lived Species. The purpose of subtracting the corrected absorption spectrum at longer time, i.e., 200 μs after the pulse (Figure 2A, curve e (▽)) from the corrected absorption spectrum at shorter time, i.e., 1 μs after the pulse (Figure 2A, curve b (○)) in Ar-saturated acetonitrile solution was to reduce the contribution of long-lived species (e.g., the hydrogenated neutral radicals of the 2,3-dihydrooxoisoaporphine (A1NH$^{\bullet}$, Chart 1)). The spectrum thus corrected represents a superposition of contributions from two major transient species: the radical anion (A1$^{\bullet-}$, Chart 1) with $\lambda_{max} = 605$ nm and the triplet (^{3}A1*) with $\lambda_{max} = 450$ nm (Figure 2B). A very good agreement between experimental and calculated spectra (Table 1) for the radical anion (A1$^{\bullet-}$, Chart 1) was found that reproduces the maximum at $\lambda_{max} = 605$ nm (black bar in Figure 2B).[7] Only a fairly good agreement between experimental and calculated spectra for the triplet (^{3}A1*) was found (Table 1); however, the more intense calculated transitions (gray bar in Figure 2B) were located within ±35 nm of the absorption experimentally observed ($\lambda_{max} = 450$ nm).[7] On the other hand, it is noteworthy that the transient absorption band with $\lambda_{max} = 450$ nm observed in flash photolysis, and assigned to the triplet of 2,3-dihydrooxoisoaporphine (^{3}A1*) (Figure 2B, curve b (○)),[7] fits very well to the absorption band with $\lambda_{max} = 450$ nm observed in pulse radiolysis (Figure 2B, curve a (□)).

5-Methoxy-2,3-dihydrooxoisoaporphine. ***Argon-Saturated Solutions.*** A transient absorption spectrum obtained 400 ns after the electron pulse in Ar-saturated acetonitrile solutions containing 0.1 mM of 5-methoxy-2,3-dihydrooxoisoaporphine (A2, Chart 1), exhibits a distinctive absorption band with $\lambda_{max} = 590$ nm, and a second much broader, and rather flat absorption band in the 400−500 nm range with two absorption maxima located at $\lambda = 420$ and 480 nm (Figure 3A, curve a (□)).

Both absorption buildups at $\lambda = 480$ and 590 nm occur within <400 ns time domain. However, the kinetic traces recorded were characterized by distinctly different time profiles; the rate of formation of the 590 nm species is slower in comparison to the 480 nm species (kinetic traces not shown). Similarly, the kinetic decays of the 480 nm and 590 nm species differ, analogous to the behavior observed in solutions containing 2,3-dihydrooxoisoaporphine.

The absorption at $\lambda = 590$ nm decays further by a relatively rapid first-order process with $k = (2.6 \pm 0.03) \times 10^5$ s^{-1} (Figure 3A, inset). However, the decay of the 480 nm transient is slower and more complex (Figure 3A, inset). It is noteworthy that, although the absorption at 480 and 590 nm decreased in intensity, the 420 nm absorption band grows further over the 7 μs time domain, with the first-order rate constant $k = (5.4 \pm 0.1) \times 10^5$ s^{-1} (Figure 3A, inset). After 7 μs, the transient spectrum is dominated by the 420 nm band (Figure 3A, curve b (○)). At the time when the 590 nm absorption disappeared, the spectrum recorded 30 μs after the pulse exhibited only a distinctive absorption band with $\lambda_{max} = 420$ nm. There was also a weak shoulder in the range 480−500 nm (Figure 3A, curve c (◇)). With the further elapse of time, the spectra observed at 60 and 300 μs after the pulse exhibit similar spectral features (Figure 3A, curves d (Δ) and e (▽)); however, a close inspection of these three spectra shows that the ratio $r = (G\epsilon_{420})/(G\epsilon_{480})$ calculated for 30, 60 and 300 μs changes, suggesting the absorption of two species.

Oxygen-Saturated Solutions. The transient absorption spectrum obtained 400 ns after the pulse consisted only of a weak absorption located at $\lambda_{max} = 420$ nm (Figure 3B, curve a (□)). It is important to note that this spectrum does not exhibit intense and distinctive absorption band with $\lambda_{max} = 590$ nm, and a second much broader, and rather flat absorption band in the 400 − 500 nm range, as the analogous absorption spectrum recorded in Ar-saturated solutions (Figure 3A, curve a (□)). This behavior can be rationalized by the complete scavenging of the precursors of 5-methoxy-2,3-dihydrooxoisoaporphine derived radical anions (A2$^{\bullet-}$, Chart 1) and triplets (^{3}A2*) that were responsible for the absorption bands suppressed. However, the resulting absorption spectrum recorded at 7 μs after the pulse is dominated by the distinctive absorption band with $\lambda_{max} = 420$ nm, and a weak shoulder in the range of 480 − 510 nm (Figure 3B, curve b (○)). For chemical reasons (radical cations are not reactive with oxygen), it has to be associated with radical cations resulting from the pulse radiolysis of 5-methoxy-2,3-dihydrooxoisoaporphine in O_2-saturated acetonitrile solutions. A fairly good agreement between the experimental and calcu-

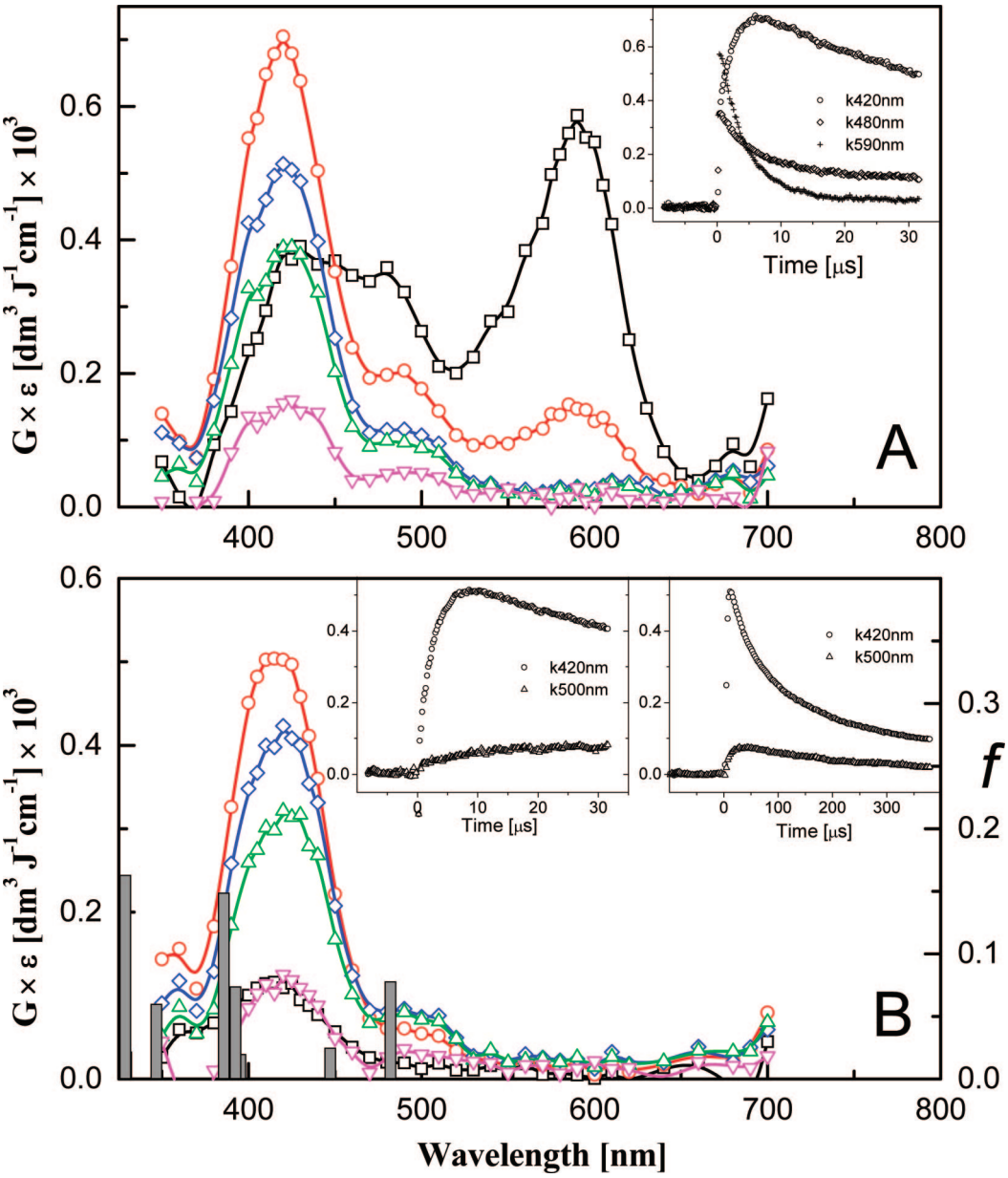

Figure 3. Absorption spectra recorded in (A) Ar-saturated, and (B) O_2-saturated acetonitrile solutions containing 0.1 mM 5-methoxy-2,3-dihydrooxoisoaporphine. Spectra were taken after the following time delays: (a) (□) 400 ns; (b) (○) 7 μs; (c) (◇) 30 μs; (d) (Δ) 60 μs; (e) (▽) 300 μs. The shaded vertical bars in panel B represent the position of the calculated electronic transitions for $A2^{\bullet+}$. The height of the bar is proportional to the oscillator strength. Inset in (A): short time profiles representing growth and/or decays at $\lambda = 420$, 480, and 590 nm. Insets in (B) short time profiles representing growth and/or decays at $\lambda = 420$ and 500 nm (left) and long time profiles representing decays at $\lambda = 420$ and 500 nm (right).

lated spectra (Table 1) for the radical cation ($A2^{\bullet+}$, Chart 1) was found. The more intense calculated electronic transitions differ by 30−35 nm; however, they reproduce quite well the main features of experimental spectra of $A2^{\bullet+}$ (Chart 1), i.e., strong electronic transitions around 400 nm (Figure 3B).

It is noteworthy that the absorption spectrum at 7 μs is very similar to the analogous spectrum recorded in Ar-saturated acetonitrile (Figure 3A, curve b (○)). Moreover, the absorption growth at $\lambda_{max} = 420$ nm is characterized by a similar time profile (Figure 3B, left inset), analogous to the time profile observed at $\lambda_{max} = 420$ nm in Ar-saturated acetonitrile (Figure 3A, inset). The kinetic trace at $\lambda = 420$ nm reached a maximum within 7 μs with k_{obs}(growth) = $(4.6 \pm 0.09) \times 10^5$ s^{-1} (Figure 3B, left inset). All these observations mentioned above suggest that in Ar-saturated acetonitrile solutions there is a significant contribution from the radical cations derived from 5-methoxy-2,3-dihydrooxoisoaporphine ($A2^{\bullet+}$, Chart 1). With the further elapse of time, the spectrum observed after 30 μs after the pulse exhibits similar spectral features (Figure 3B, curve c (◇)); however, a close inspection of both spectra shows that a ratio $r = (G\epsilon_{420})/(G\epsilon_{500})$ calculated for 7 and 30 μs changes. This is consistent with the observation that the 420 and 500 nm kinetic traces recorded within 35 μs (Figure 3B, left inset) and 375 μs time windows (Figure 3B, right) were characterized by distinctly different time profiles, On the other hand, for example, the kinetic trace at $\lambda = 420$ nm represents a decay within the 7−35 μs range. On the other hand, within the similar time range the kinetic trace at $\lambda = 500$ nm represents a growth with k_{obs}(growth) = $(1.1 \pm 0.1) \times 10^5$ s^{-1} (Figure 3B, left inset) analogous to the behavior observed in solution of 2,3-dihydrooxoisoaporphine for 350 nm and 500 nm kinetic traces (Figure 1B, left inset). By analogy to 2,3-dihydrooxoisoapor-

phine, this behavior can be again rationalized by the existence of two distinct radical cationic species. The absorption spectra recorded 60 (Figure 3B, curve d (Δ)) and 300 μs (Figure 3B, curve e (▽)) after the pulse exhibited a similar spectral features; however, the ratio $r = (G\epsilon_{420})/(G\epsilon_{500})$ calculated for 60 and 300 μs does not change, suggesting the existence of one radical cationic species or two radical cationic species being in equilibrium, likely the radical cation and the dimeric species $(A2)_2^{\bullet+}$ at a constant molar proportion.

Corrected Spectra To Eliminate Contribution of Radical Cation Species. Elimination of the contribution of radical cation species to the observed absorption spectra in Ar-saturated acetonitrile containing A2 is necessary, in particular, because the absorption of radical cations derived from 5-methoxy-2,3-dihydrooxoisoaporphine ($A2^{\bullet+}$, Chart 1)) is much more pronounced than the absorption of radical cations derived from 2,3-dihydrooxoisoaporphine ($A1^{\bullet+}$, Chart 1). Moreover, the absorption spectrum of $A2^{\bullet+}$ (Chart 1) is red-shifted. Therefore, it overlaps substantially and, as a consequence, distorts absorption spectra in the region where radical anions ($A2^{\bullet-}$, Chart 1) and triplets ($^3A2^*$) absorb. The corrected spectrum recorded 400 ns after the pulse represents combined absorption bands of at least two different species: a radical anion ($A2^{\bullet-}$, Chart 1) with $\lambda_{max} =$ 590 nm and possibly a triplet ($^3A2^*$) (Figure 4A, curve a (□)).

The position of the absorption maximum of the radical anion ($A2^{\bullet-}$, Chart 1) is in reasonably good agreement with the predicted electronic transitions for the radical anion ($A2^{\bullet-}$) (vide infra Figure 4B and Table 1) calculated by the ZINDO/S-PM3 method.[7] However, a broad 480 nm absorption band with a well pronounced 420 nm shoulder deserves more careful analysis. Because the rate of the decay of $A2^{\bullet-}$ (Chart 1) is faster in comparison to the rate of decay of $A1^{\bullet-}$ (Chart 1) (vide supra), the contribution of the neutral-hydrogenated radicals (A2NH$^\bullet$, Chart 1)) should be even much more pronounced in the absorption spectra, observed at shorter times. This conclusion is confirmed by the observation of absorption spectra recorded after 7 μs (Figure 4A, curve b (○)) and longer times (Figure 4A, curves c (◇)−e (▽)). These spectra consisted of two absorption bands, one at $\lambda = 420$ nm and a second at $\lambda = 480$ nm. They exhibit the same spectral features as the spectrum generated in this work by means of the laser flash photolysis of acetonitrile solutions containing 5-methoxy-2,3-dihydrooxoisoaporphine (A2, Chart 1) in the presence of triethylamine (TEA) (Figure 4A, inset). On the basis of our earlier mechanism of photoreduction of oxoisoaporphines,[7] they were assigned to the neutral-hydrogenated radicals (A2NH$^\bullet$, Chart 1). Similarly, as for the neutral-hydrogenated radical A1NH$^\bullet$ (Chart 1), the calculated electronic transitions reproduce only fairly well (Table 1) the main features of the experimental spectrum, i.e., the presence of two separated absorption bands, one with the maximum located in the UV, and the second one in the visible region (Figure 4A bars).

Corrected Spectra To Eliminate Contribution of Long-Lived Species. Because the corrected absorption spectrum (without contribution of radical cation species, Figure 4A, curve a (□)), even at short times after the pulse, is "contaminated" by the presence of the radical A2NH$^\bullet$ (Chart 1), the same approach, as used for 2,3-dihydrooxoisoaporphine to eliminate its contribution, was applied. Therefore, the corrected spectrum at 7 μs (Figure 4A, curve b (○)), when most of the triplets $^3A2^*$ disappeared, was subtracted from the corrected spectrum at 400 ns (Figure 4A, curve a (□)). The resultant spectrum represents now a superposition of contributions from two major transient species: the radical anion ($A2^{\bullet-}$, Chart 1) with $\lambda_{max} = 590$ nm, and the triplet ($^3A2^*$) with $\lambda_{max} = 440$ nm, however, still with a low contribution from the radical A2NH$^\bullet$ (Chart 1) (Figure 4B, curve a (□)). Evidence for the formation of $^3A2^*$ is seen in the formation of a transient absorption band with $\lambda_{max} = 440$ nm in laser flash photolysis studies,[7] which was assigned to the triplet of 5-methoxy-2,3-dihydrooxoisoaporphine ($^3A2^*$) (Figure 4B, curve b (○)). It is noteworthy that a very good agreement between experimental and calculated spectra for the triplet ($^3A2^*$) was found that reproduces the strongest electronic transition at $\lambda_{max} = 440$ nm (Table 1). Furthermore, the calculated spectrum for the radical anion ($A2^{\bullet-}$, Chart 1) reproduces reasonably well (Table 1) the spectrum observed experimentally with $\lambda_{max} = 590$ nm (Figure 4B).

Semiempirical Quantum Mechanics Calculations. The most relevant spectroscopically active electronic transitions along with the oscillator-strengths for the radical anions ($A1^{\bullet-}$ and $A2^{\bullet-}$),

TABLE 1: Spectral Parameters of the Excited Triplet States ($^3A^*$), Radical Anions ($A^{\bullet-}$), Radical Cations ($A^{\bullet+}$), and Neutral-Hydrogenated Radicals (ANH$^\bullet$) Derived from 2,3-Dihyrooxoisoaporphine (A1) and 5-Methoxy-2,3-dihydrooxoisoaporphine (A2) Calculated by the ZINDO/S-PM3 Method

	transients							
	$^3A^*$ [a]		$A^{\bullet-}$ [a]		$A^{\bullet+}$ [b]		ANH$^\bullet$ [a]	
oxoisoaporphine (A)	λ (nm)	f	λ (nm)	f	λ (nm)	f	λ (nm)	f
A1	868.2	0.050	860.8	0.050	417.7	0.057	**538.0**	**0.075**
	655.2	0.006	**616.0**	**0.212**	397.6	0.007	497.3	0.002
	585.3	0.031	441.4	0.032	**392.0**	**0.078**	478.0	0.033
	495.1	**0.103**	439.0	0.001	378.4	0.013	416.6	0.012
	421.4	**0.605**	385.1	0.051	372.9	0.034	384.5	0.005
	416.5	0.037	361.3	0.065	332.6	0.018	376.9	0.020
	371.1	0.015	**343.2**	**0.136**	**329.0**	**0.200**	**362.0**	**0.157**
					325.0	**0.219**	350.1	0.003
A2	883.7	0.021	882.0	0.049	**482.0**	**0.078**	**552.0**	**0.079**
	634.2	**0.095**	**624.3**	**0.216**	447.2	0.025	512.9	0.001
	592.5	0.011	447.8	0.033	**395.2**	0.020	500.3	0.014
	487.7	**0.094**	446.3	0.001	**392.4**	**0.074**	422.4	0.004
	440.7	**0.634**	387.0	0.058	**385.7**	**0.149**	382.6	0.027
	424.8	0.016	366.6	0.011	346.8	0.060	**373.9**	**0.254**
	380.3	0.023	**343.8**	**0.221**	329.3	0.022	368.2	0.023
					328.8	0.063	352.0	0.004

[a] From ref 7. [b] This work.

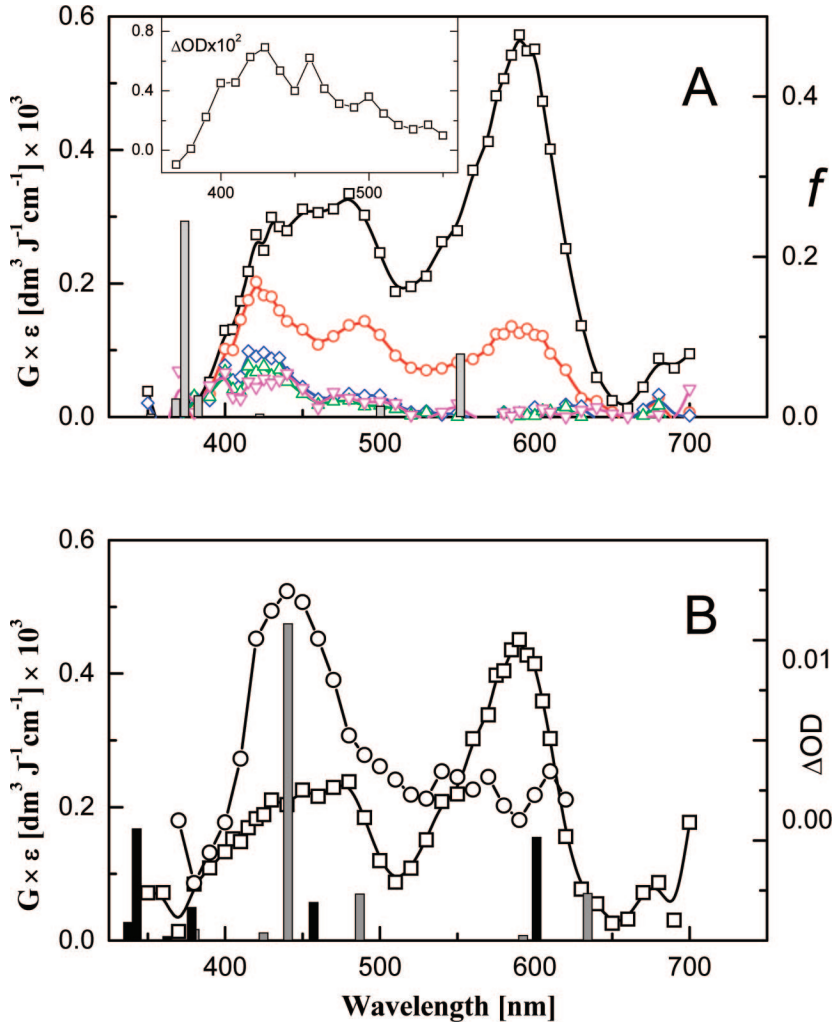

Figure 4. (A) Absorption spectra from the subtraction of the absorption spectra obtained in O_2-saturated solutions from the respective absorption spectra obtained in Ar-saturated solutions at different time delays: (a) (□) 400 ns; (b) (○) 7 μs; (c) (◇) 30 μs; (d) (Δ) 60 μs; (e) (▽) 300 μs. The shaded vertical bars represent the position of the calculated electronic transitions for A2NH$^{\bullet}$. The height of the bar is proportional to the oscillator strength. Inset: absorption spectrum of the neutral-hydrogenated radical (A2NH$^{\bullet}$) obtained by flash photolysis of 5-methoxy-2,3-dihydrooxoisoaporphine in N_2-saturated acetonitrile solutions (□). (B) Absorption spectrum from the subtraction of the corrected absorption spectrum at 7 μs (from the panel A) from the corrected absorption spectrum at 1 μs (from the panel A) (□) and absorption spectrum of the 5-methoxy-2,3-dihydrooxoisoaporphine triplet (^{32}A*) obtained by flash photolysis of 5-methoxy-2,3-dihydrooxoisoaporphine in N_2-saturated acetonitrile solutions (○).[7] The vertical bars represent the position of the electronic transition for ^{3}A2* (gray bar) and A2$^{\bullet-}$ (black bar). The height of the bar is proportional to the oscillator strength.

triplets (^{3}A1* and ^{3}A2*), and neutral-hydrogenated radicals (A1NH$^{\bullet}$ and A2NH$^{\bullet}$) were calculated in our earlier work.[7] For the purpose of this work, the spectroscopically relevant active transitions, at the wavelengths <300 nm had to be calculated for the radical cations of two oxoisoaporphines (A1 and A2). They are summarized in Table 1 together with the respective data calculated earlier by us for three other types of transients (A$^{\bullet-}$, ^{3}A*, and ANH$^{\bullet}$) which were also generated by pulse radiolysis.

Discussion

The present work reports for the first time on spectral data regarding the radical anions and radical cations derived from two oxoisoaporphines, i.e., 2,3-dihydrooxoisoaporphine and 5-methoxy-2,3-dihydrooxoisoaporphine. In addition, the kinetics of formation and decay of these transients were presented.

Radical Anions. The observed maxima for radical anions of 2,3-dihydrooxoisoaporphine (λ_{max} = 605 nm) and of 5-methoxy-2,3-dihydrooxoisoaporphine (λ_{max} = 590 nm) are in general agreement with the results of the ZINDO/S semiempirical quantum mechanical calculations.[7] It has to be noted that the methoxy group (−OCH_3) at position 5 in the aromatic ring influences slightly the position of the maximum by shifting it to the shorter wavelengths as compared with that observed for the nonsubstituted 2,3-dihydrooxoisoaporphine. This might suggest a partial delocalization of the negative charge into the aromatic ring.

The radical anions can be formed either by a direct attachment of the solvated electron (eq 12) or by an electron transfer from the acetonitrile radical anion to oxoisoaporphine (eq 13).

$$e^-_{solv} + A1/A2 \rightarrow A1^{\bullet-}/A2^{\bullet-} \quad (12)$$

$$CH_3CN^{\bullet-} + A1/A2 \rightarrow CH_3CN + A1^{\bullet-}/A2^{\bullet-} \quad (13)$$

The molar absorption coefficients at the respective maxima of radical anions were calculated to be ϵ_{605} = 5600 M^{-1} cm^{-1}, and ϵ_{590} = 4900 M^{-1} cm^{-1} for A1$^{\bullet-}$ and A2$^{\bullet-}$, respectively, taking the *G*-value of the reducing species of 1.03 (0.1067 μM

J^{-1}) measured in acetonitrile.[18] These relatively high values of molar absorption coefficients are in line with the calculated oscillator strengths at the respective maxima of radical anions, $A1^{\bullet -}$ and $A2^{\bullet -}$ (Table 1).

Because the long-lived absorptions observed at longer time scales in corrected spectra (without any contribution from the cationic species) were assigned to the respective neutral-hydrogenated radicals ($A1NH^{\bullet}$ and $A2NH^{\bullet}$), this implies that both radical anions $A1^{\bullet -}$ and $A2^{\bullet -}$ decay predominantly through protonation. Moreover, because the decays of radical anions are strictly of first-order with k-values lying in the range of 10^5 s^{-1}, this also implies that protonation could occur via reaction with the adventitious water molecules present in the solvent (eq 14):

$$A1^{\bullet -}/A2^{\bullet -} + H_2O \rightarrow A1NH^{\bullet}/A2NH^{\bullet} + OH^- \qquad (14)$$

The reason the protonation by water molecules is relatively fast may be sought in the fact that the radical anions of oxoisoaporphines might have large dipole moments. This phenomenon can be rationalized by a larger localization of the negative charge on the nitrogen atom. Our observation regarding the increase in the protonation rate constant from 1.5×10^5 s^{-1} for $A1^{\bullet -}$ to 2.6×10^5 s^{-1} for $A2^{\bullet -}$ is in line with the calculated dipole moments 2.328 and 5.336 D for $A1^{\bullet -}$ and $A2^{\bullet -}$, respectively. The correlation of radical anion decay rate by protonation with dipole moments has also been observed for geometric isomers of stilbene,[33] and terphenyl,[34] where the radical anions of bent isomers have been shown to decay faster by protonation.

Radical Cations. A substantial influence of the substitution in the aromatic ring on the position of the maxima of the absorption bands that were assigned to radical cations was observed. In O_2-saturated acetonitrile, the radical cation derived from 2,3-dihydrooxoisoaporphine ($A1^{\bullet +}$) shows its principal absorption maximum at $\lambda \leq 350$ nm. On the other hand, the radical cation derived from 5-methoxy-2,3-dihydrooxoisoaporphine ($A2^{\bullet +}$), in the same conditions, shows the maximum at $\lambda = 420$ nm. The significant red shift of the absorption maximum can be rationalized by an increase of charge density due to the presence of a methoxy group. These experimental observations were confirmed by the ZINDO/S calculations of the most intense absorptions for $A2^{\bullet +}$. They were found to be red-shifted by about 60 nm with respect to those of 2,3-dihydrooxoisoaporphine (Table 1).

The radical cations can be formed by charge transfer from the acetonitrile radical cation to oxoisoaporphine (eq 15).

$$CH_3CN^{\bullet +} + A1/A2 \rightarrow CH_3CN + A1^{\bullet +}/A2^{\bullet +} \qquad (15)$$

On the basis of the previously measured lifetime of the radical cation of acetonitrile ($\tau \approx 10$ μs),[14] and taking the respective pseudo-first-order rate constants measured for the formation of $A1^{\bullet +}$/ $A2^{\bullet +}$ (vide supra), the rate constants for reaction 15 were estimated to be 2.8×10^9 and 3.6×10^9 M^{-1} s^{-1}, respectively. These values are slightly higher than the value measured for the analogous reaction involving retinal (7.4×10^8 M^{-1} s^{-1}).[14] This might suggest that ionization potentials of oxoisoaporphines derivatives are lower than the respective ionization potential of retinal. It should be also noted that the formation of radical cations of oxoisoaporphines ($A1^{\bullet +}/A2^{\bullet +}$) takes place with slower kinetics in comparison to the formation kinetics of the respective radical anions ($A1^{\bullet -}/A2^{\bullet -}$) and remains essentially unchanged upon O_2 saturation. This observation is in agreement with previous pulse radiolysis studies of radical ions derived from retinal in acetonitrile.[14] The formation of the radical cations derived from retinal was also slower than the formation due to the radical anion and also remained unchanged in O_2-saturated solutions.

Triplet Excited States. The observation of triplet excited states $^3A1^*$ and $^3A2^*$ is in agreement with earlier studies demonstrating formation of triplet excited states of acetonitrile ($^3CH_3CN^*$).[22,30] The observed absorption maxima for triplets of 2,3-dihydrooxoisoaporphine ($^3A1^*$) ($\lambda_{max} = 450$ nm) and of 5-methoxy-2,3-dihydrooxoisoaporphine ($^3A2^*$) ($\lambda_{max} = 440$ nm) generated by pulse radiolysis are in excellent agreement with the absorption maxima for the respective triplets generated by laser flash photolysis. The triplets can be formed by energy transfer from the acetonitrile triplet excited state to oxoisoaporphine (eq 16):

$$^3CH_3CN^* + A1/A2 \rightarrow CH_3CN + {}^3A1^*/{}^3A2^* \qquad (16)$$

Taking the G-value of the $^3CH_3CN^*$ of $\sim$0.3 ($\sim$0.03 μM J^{-1}) measured in acetonitrile[30] together with the corrected $G\epsilon$ values for $^3A1^*$ and $^3A2^*$ at the respective wavelengths (from Figures 2B and 4B), the molar absorption coefficients of triplets can be estimated: $\epsilon_{450} = 9000$ M^{-1} cm^{-1} and $\epsilon_{440} = 6700$ M^{-1} cm^{-1} for $^3A1^*$ and $^3A2^*$, respectively. These relatively high values are in line with the calculated oscillator strengths at the respective maxima of triplet excited states, $^3A1^*$ and $^3A2^*$ (Table 1). Because the absorption spectra of $^3A1^*/^3A2^*$ overlap with the absorption spectra of other transients formed in acetonitrile ($A1NH^{\bullet}$/ $A2NH^{\bullet}$ and $A1^{\bullet +}/A2^{\bullet +}$), it was not possible to follow either their formation or decay kinetics.

Conclusions

In the current paper, application of pulse radiolysis as a complementary method of generation of radical ions allowed selective generation and observation of radical anions and cations of two oxoisoaporphine derivatives, 2,3-dihydrooxoisoaporphine (2,3-DHOA) and 5-methoxy-2,3-dihydrooxoisoaporphine (5-MeO-2,3-DHOA). The experimental spectra of the "isolated" radical anions were reproduced adequately by semiempirical quantum mechanical calculations performed previously using ZINDO/S on the optimized PM3 geometry. Such comparison was not possible when radical anions were generated photochemically and were always paired with the radical cation of the amine.

Our current findings, especially those addressing radical ions, support strongly the photoreduction mechanism of 2,3-dihydrooxoisoaporphines previously reported. Moreover, they will be useful for interpretation of spectral data obtained during photooxidation of oxoisoaporphine dyes currently in progress.

Acknowledgment. We thank FONDECYT grants Nos. 1070623, 7070295 and 7060244 for the financial support which made possible exchange scientific visits of J.R.F. and K.B. in the INCT (Warsaw, Poland) and the Universidad de Chile (Santiago, Chile), respectively.

References and Notes

(1) Sugimoto, Y.; Babiker, H. A. A.; Inanaga, S.; Kato, M.; A., I. *Phytochemistry* **1999**, *52*, 1431–1435.

(2) Yu, B. W.; Meng, L. H.; Chen, J. Y.; Zhou, T. X.; Cheng, K. F.; Ding, J.; Qin, G. W. *J. Nat. Prod.* **2001**, *64*, 968–970.

(3) Hu, S.; Xu, S.; Yao, X.; Cui, C.; Tezuka, Y.; Kikuchi, T. *Chem. Pharm. Bull.* **1993**, *41*, 1866–1868.

(4) Hou, C.; Xue, H. *Acta Pharm. Sin.* **1985**, *20*, 112–117.

(5) Flors, C.; Santi Nonell, S. *Acc. Chem. Res.* **2006**, *39*, 293–300.

(6) De la Fuente, J. R.; Jullian, C.; Saitz, C.; Sobarzo-Sanchez, E.; Neira, V.; Gonzalez, C.; Lopez, R.; Pessoa-Mahana, H. *Photochem. Photobiol. Sci.* **2004**, *3*, 194–199.

(7) De la Fuente, J. R.; Neira, V.; Saitz, C.; Jullian, C.; Sobarzo-Sanchez, E. *J. Phys. Chem. A.* **2005**, *109*, 5897–5904.

(8) De la Fuente, J. R.; Jullian, C.; Saitz, C.; Neira, V.; Poblete, O.; Sobarzo-Sanchez, E. *J. Org. Chem.* **2005**, *70*, 8712–8716.

(9) Karolczak, S. *Pulse radiolysis - experimental features*; Mayer, J., Ed.; Polish Scientific Publishers, PWN: Warszawa, 1999; pp 11−37.

(10) Matheson, M. S.; Dorfman, L. *Pulse radiolysis*; MIT Press: Cambridge, MA, 1969.

(11) Ebert, M.; Keene, J. P.; Swallow, A. J.; Baxendale, J. H. *Pulse radiolysis*; Academic Press: New York, 1965.

(12) Raghavan, N. V.; Das, P. K.; Bobrowski, K. *J. Am. Chem. Soc.* **1981**, *103*, 4569–4573.

(13) Bobrowski, K.; Das, P. K. *J. Phys. Chem.* **1985**, *89*, 5079–5085.

(14) Bobrowski, K.; Das, P. K. *J. Phys. Chem.* **1985**, *89*, 5733–5738.

(15) Bobrowski, K.; Dzierøkowska, G.; Grodkowski, J.; Stuglik, Z.; Zagórski, Z. P.; McLaughlin, W. L. *J. Phys. Chem.* **1985**, *89*, 4358–4366.

(16) Bobrowski, K.; Das, P. K. *J. Phys. Chem.* **1987**, *91*, 1210–1215.

(17) Tran-Thi, T. H.; Koulkes-Pujo, A. M.; Gilles, L.; Genies, M.; Sutton, J. *Radiat. Phys. Chem.* **1980**, *15*, 209–214.

(18) Bell, I. P.; Rodgers, M. A. J.; Burrows, H. D. *J. Chem. Soc., Faraday Trans.1* **1977**, *73*, 315–326.

(19) Burrows, H. D.; Kosower, E. M. *J. Phys. Chem.* **1974**, *78*, 112–117.

(20) Baptista, J. L.; Burrows, H. D. *J. Chem. Soc., Faraday Trans. 1* **1974**, *70*, 2066–2079.

(21) Ayscough, P. B.; Drawe, H.; Kohler, P. *Radiat. Res.* **1968**, *33*, 263–273.

(22) Singh, A.; Gesser, H. D.; Scott, A. R. *Chem. Phys. Lett.* **1968**, *2*, 271–273.

(23) Fabre, J. L.; Farge, D.; James, C. *Dibenzo[de.h]quinoline derivatives*: USA, 1978.

(24) Walker, G. N.; Kempton, R. J. *J. Org. Chem.* **1971**, *36*, 1413–1416.

(25) Sobarzo-Sanchez, E. Sintesis y Reactividad en el Ambitode las 7H-Dibenzo(de,h)quinolinas. Universidad de Chile, 2003.

(26) Mirkowski, J.; Wisniowski, P.; Bobrowski, K. INCT Annual Report 2000; INCT: **2001**.

(27) Bobrowski, K. *Nukleonika* **2005**, *50* (3), S67–S76.

(28) De la Fuente, J. R.; Cañete, A.; Saitz, C.; Jullian, C. *J. Phys. Chem. A* **2002**, *106*, 7113–7120.

(29) Viteri, G.; Edwards, A. M.; De la Fuente, J. R.; Silva, E. *Photochem. Photobiol.* **2003**, *77*, 535–540.

(30) Hayon, E. *J. Chem. Phys.* **1970**, *53*, 2353–2358.

(31) Vedeneyev, V. I.; Gurvich, L. V.; Kondrat'yev, V. N.; Medvedev, V. A.; Frankevich, Y. L. *Bond energies, ionization potentials and electron affinities*; Edward Arnold Ltd.: London, 1966.

(32) Bobrowski, K.; Das, P. K. *J. Phys. Chem.* **1986**, *90*, 927–931.

(33) Levanon, H.; Neta, P. *Chem. Phys. Lett.* **1977**, *48*, 345–349.

(34) Arai, S.; Tremba, E. L.; Brandon, J. R.; Dorfman, L. M. *Can. J. Chem.* **1967**, *45*, 1119–1123.